Newton-Multigrid Least-Squares FEM for S-V-P Formulation of the Navier-Stokes Equations

A. Ouazzi, M. Nickaeen, S. Turek, and M. Waseem

Institut für Angewandte Mathematik, LSIII, TU Dortmund, Vogelpothsweg 87, D-44227 Dortmund, Germany*

Abstract. Least-squares finite element methods are motivated, beside others, by the fact that in contrast to standard mixed finite element methods, the choice of the finite element spaces is not subject to the LBB stability condition and the corresponding discrete linear system is symmetric and positive definite. We intend to benefit from these two positive attractive features, on one hand, to use different types of elements representing the physics as for instance the jump in the pressure for multiphase flow and mass conservation and, on the other hand, to show the flexibility of the geometric multigrid methods to handle efficiently the resulting linear systems. With the aim to develop a solver for non-Newtonian problems, we introduce the stress as a new variable to recast the Navier-Stokes equations into first order systems of equations. We numerically solve S-V-P, Stress-Velocity-Pressure, formulation of the incompressible Navier-Stokes equations based on the least-squares principles using different types of finite elements of low as well as higher order. For the discrete systems, we use a conjugate gradient (CG) solver accelerated with a geometric multigrid preconditioner. In addition, we employ a Krylov space smoother which allows a parameter-free smoothing. Combining this linear solver with the Newton linearization results in a robust and efficient solver. We analyze the application of this general approach, of using different types of finite elements, and the efficiency of the solver, geometric multigrid, throughout the solution of the prototypical benchmark configuration 'flow around cylinder'.

Key words: Least-Squares EFM, multigrid, S-V-P formulation, mass conservation, Navier-Stokes equations.

1 Introduction

Least-Squares FEM (LSFEM) is generally motivated by the desire to recover the advantageous features of Rayleigh-Ritz methods, as for instance, the choice of the approximation spaces is free from discrete compatibility conditions and the corresponding discrete system is symmetric and positive definite [4].

* *Email addresses*: `Abderrahim.Ouazzi@math.tu-dortmund.de` (A. Ouazzi), `masoud.nickaeen@rutgers.edu` (M. Nickaeen), `ture@featflow.de` (S. Turek), `Muhammad.Waseem@math.tu-dortmund.de` (M. Waseem)

In this paper, we solve the incompressible Navier-Stokes (NS) equations with LSFEM. Direct application of the LSFEM to the second-order NS equations requires the use of quite impractical C^1 finite elements [4]. Therefore, we introduce the stress as a new variable, on one hand to recast the Navier-Stokes equations to a first-order system of equations, and on the other hand to develop the basic solver for non-newtonian problems, i.e. the stress-velocity-pressure (S-V-P) formulation.

The resulting LSFEM system is symmetric and positive definite [4]. This permits the use of the conjugate gradient (CG) method and efficient multigrid solvers for the solution of the discrete system. In order to improve the efficiency of the solution method, the multigrid and the Krylov subspace method, here CG, can be combined with two different strategies. The first strategy is to use the multigrid as a preconditioner for the Krylov method [1]. The advantage of this scheme is that the Krylov method reduces the error in eigenmodes that are not being effectively reduced by multigrid. The second strategy is to employ Krylov preconditions methods as multigrid smoother. The Krylov methods appropriately determine the size of the solution updates at each smoothing step. This leads to smoothing sweeps which, in contrast to the standard SOR or Jacobi smoothing, are free from predefined damping parameters.

We develop a geometric multigrid solver as a preconditioner for the CG (MPCG) iterations to solve the S-V-P system with LSFEM. The MPCG solver has been first introduced and successfully used by the authors for the solution of the vorticity-based Navier-Stokes equations [3]. We use a CG pre/post-smoother to obtain efficient and parameter-free smoothing sweeps. We demonstrate a robust and grid independent behavior for the solution of different flow problems with both bilinear and biquadratic finite elements. Moreover, we show through the 'flow around cylinder' benchmark that accurate results can be obtained with LSFEM provided that higher order finite elements are used.

Therefore, the paper is organized as follows: in the next section we introduce the incompressible NS equations, the Newton linearization, the continuous and the discrete least-square principles with their properties and the designed LSFEM solver. In the next section, we present the general MPCG solver settings and the detailed results of the flow parameters in the 'flow around cylinder' problem. Finally, we give a conclusion and an outlook in the last section.

2 LSFEM for the Navier-Stokes Equations

The incompressible NS equations for a stationary flow are given by

$$\begin{cases} \boldsymbol{u} \cdot \nabla \boldsymbol{u} + \nabla p - \nu \triangle \boldsymbol{u} = f & \text{in } \Omega \\ \nabla \cdot \boldsymbol{u} = 0 & \text{in } \Omega \\ \boldsymbol{u} = \boldsymbol{g}_D & \text{on } \Gamma_D \\ \boldsymbol{n} \cdot \boldsymbol{\sigma} = \boldsymbol{g}_N & \text{on } \Gamma_N \end{cases} \tag{1}$$

where $\Omega \subset \mathbb{R}^2$ is a bounded domain, p is the normalized pressure $p = P/\rho$, $\nu = \mu/\rho$ is the kinematic viscosity, f is the source term, $\boldsymbol{g}_D$ is the value of the Dirichlet boundary conditions on the Dirichlet boundary Γ_D, $\boldsymbol{g}_N$ is the prescribed traction on the Neumann boundary $\boldsymbol{\Gamma}_N$, $\boldsymbol{n}$ is the outward unit normal on the boundary, $\boldsymbol{\sigma}$ is the stress tensor and $\Gamma = \Gamma_D \cup \Gamma_N$ and $\Gamma_D \cap \Gamma_N = \emptyset$. The kinematic viscosity and the density of the fluid are assumed to be constant. The first equation in (1) is the momentum equation where velocities $\boldsymbol{u} = [u\,,\,v]^T$ and pressure p are the unknowns and the second equation represents the continuity equation.

2.1 First-order Stress-Velocity-Pressure System

The straightforward application of the LSFEM to the second-order NS equations requires C^1 finite elements [4]. To avoid the practical difficulties in the implementation of such FEM, we first recast the second-order equation to a system of first-order equations. Another important reason for not using the straightforward LSFEM is that the resulting system matrix will be ill-conditioned.

To derive the S-V-P formulation, the Cauchy stress, $\boldsymbol{\sigma}$, is introduced as a new variable

$$\boldsymbol{\sigma} = 2\nu \mathbf{D}(\boldsymbol{u}) - p\mathbf{I} \tag{2}$$

where $2\mathbf{D} := \nabla + \nabla^T$. Using the NS equations and the stress equation (2) we obtain the first-order Stress-Velocity-Pressure (S-V-P) system of equations

$$\begin{cases} \boldsymbol{u} \cdot \nabla \boldsymbol{u} - \nabla \cdot \boldsymbol{\sigma} = f & \text{in } \Omega \\ \nabla \cdot \boldsymbol{u} = 0 & \text{in } \Omega \\ \boldsymbol{\sigma} + p\mathbf{I} - 2\nu \mathbf{D}(\boldsymbol{u}) = 0 & \text{in } \Omega \\ \boldsymbol{u} = \boldsymbol{g}_D & \text{on } \Gamma_D \\ \boldsymbol{n} \cdot \boldsymbol{\sigma} = \boldsymbol{g}_N & \text{on } \Gamma_N \end{cases} \tag{3}$$

2.2 Continuous Least-squares Principle

We introduce the spaces of admissible functions based on the residuals of the first-order system (3)

$$V := \mathbf{H}(\mathrm{div}, \Omega) \cap \mathbf{H}^s(\Omega) \times \mathbf{H}^1_{g_D,D}(\Omega) \times L^2_0(\Omega) \tag{4}$$

and we define the S-V-P least-squares energy functional in the L^2-norm

$$\begin{aligned} \mathcal{J}(\boldsymbol{\sigma}, \boldsymbol{u}, p; f) = & \frac{1}{2} \bigg(\int_\Omega |\boldsymbol{\sigma} + p\mathbf{I} - 2\nu \mathbf{D}(\boldsymbol{u})|^2 \, d\Omega \\ & + \int_\Omega |\nabla \cdot \boldsymbol{u}|^2 \, d\Omega + \int_\Omega |\boldsymbol{u} \cdot \nabla \boldsymbol{u} + \nabla \cdot \boldsymbol{\sigma} - f|^2 \, d\Omega \\ & + \int_{\Gamma_N} |\boldsymbol{n} \cdot \boldsymbol{\sigma} - \boldsymbol{g}_N|^2 \, ds \bigg) \qquad \forall (\boldsymbol{\sigma}, \boldsymbol{u}, p) \in V \end{aligned} \tag{5}$$

where we have assumed extra regularity for the stress to define the functional on the boundary Γ_N in $L^2(\Gamma_N)$. The minimization problem associated with the least-squares functional in (5) is to find $\tilde{\boldsymbol{u}} \in \boldsymbol{V}$, $\tilde{\boldsymbol{u}} := (\boldsymbol{\sigma}, \boldsymbol{u}, p)$, such that

$$\tilde{\boldsymbol{u}} = \underset{\tilde{\boldsymbol{v}} \in V}{\operatorname{argmin}} \mathcal{J}(\tilde{\boldsymbol{v}}; f) \tag{6}$$

2.3 Newton Linearization

The S-V-P system (3) is nonlinear, due to the presence of the convective term, $\boldsymbol{u} \cdot \nabla \boldsymbol{u}$, in the momentum equation. Let $\mathcal{R}$ denote the residuals for the S-V-P system (3). We use the Newton method to approximate the nonlinear residuals. The nonlinear iteration is updated with the correction $\delta\tilde{\boldsymbol{u}}$, $\tilde{\boldsymbol{u}}^{k+1} = \tilde{\boldsymbol{u}}^k + \delta\tilde{\boldsymbol{u}}$. Then, the Newton linearization gives the following approximation for the residuals:

$$\begin{aligned} \mathcal{R}(\tilde{\boldsymbol{u}}^{k+1}) =& \mathcal{R}(\tilde{\boldsymbol{u}}^k + \delta\tilde{\boldsymbol{u}}) \\ \simeq& \mathcal{R}(\tilde{\boldsymbol{u}}^k) + \left[\frac{\partial \mathcal{R}(\tilde{\boldsymbol{u}}^k)}{\partial x}\right] \delta\tilde{\boldsymbol{u}} \end{aligned} \tag{7}$$

Using the least-squares principle, the resulting quadratic linearized functional, $\mathcal{L}$, is given in terms of L^2-norms as:

$$\mathcal{L}(\boldsymbol{u}^k; \delta\tilde{\boldsymbol{u}}) = \frac{1}{2} \int_{\Omega} \left| \mathcal{R}(\tilde{\boldsymbol{u}}^k) + \left[\frac{\partial \mathcal{R}(\tilde{\boldsymbol{u}}^k)}{\partial x}\right] \delta\tilde{\boldsymbol{u}} \right|^2 d\Omega \tag{8}$$

where we omitted the residual on the Neumann boundary for alluding briefly the main points. Minimizing the quadratic linearized functional (8) is equivalent to find $\delta\tilde{\boldsymbol{u}}$ such that:

$$\int_{\Omega} \left(\mathcal{R}(\tilde{\boldsymbol{u}}^k) + \left[\frac{\partial \mathcal{R}(\tilde{\boldsymbol{u}}^k)}{\partial x}\right] \delta\tilde{\boldsymbol{u}} \right) \cdot \left(\left[\frac{\partial \mathcal{R}(\tilde{\boldsymbol{u}}^k)}{\partial x}\right] \tilde{\boldsymbol{v}} \right) d\Omega = 0 \quad \forall \tilde{\boldsymbol{v}} \tag{9}$$

In the operator form, let $\mathcal{A}$ and $\mathcal{F}$ defined as follows:

$$\mathcal{A}(\tilde{\boldsymbol{u}}^k) := \left[\frac{\partial \mathcal{R}(\tilde{\boldsymbol{u}}^k)}{\partial x}\right]^* \left[\frac{\partial \mathcal{R}(\tilde{\boldsymbol{u}}^k)}{\partial x}\right], \quad \mathcal{F}(\tilde{\boldsymbol{u}}^k) := -\left[\frac{\partial \mathcal{R}(\tilde{\boldsymbol{u}}^k)}{\partial x}\right]^* \mathcal{R}(\tilde{\boldsymbol{u}}^k). \tag{10}$$

Then, the linear system to solve at each nonlinear iteration is:

$$\mathcal{A}(\tilde{\boldsymbol{u}}^k)\delta\tilde{\boldsymbol{u}} = \mathcal{F}(\tilde{\boldsymbol{u}}^k) \tag{11}$$

The resulting Newton iteration for the least-squares formulation is given as follows:

$$\tilde{\boldsymbol{u}}^{k+1} = \tilde{\boldsymbol{u}}^k - \left(\left[\frac{\partial \mathcal{R}(\tilde{\boldsymbol{u}}^k)}{\partial x}\right]^* \left[\frac{\partial \mathcal{R}(\tilde{\boldsymbol{u}}^k)}{\partial x}\right] \right)^{-1} \left[\frac{\partial \mathcal{R}(\tilde{\boldsymbol{u}}^k)}{\partial x}\right]^* \mathcal{R}(\tilde{\boldsymbol{u}}^k) \tag{12}$$

2.4 Variational Formulation

The variational formulation problem based on the optimality condition of the minimization problem (6), considering the Newton Linearization in (2.3), reads

$$\begin{cases} Find\,(\boldsymbol{\sigma}, \boldsymbol{u}, p) \in V \quad s.t. \\ \langle \mathcal{A}(\boldsymbol{\sigma}, \boldsymbol{u}, p), (\boldsymbol{\tau}, \boldsymbol{v}, q) \rangle = \mathcal{F}(\boldsymbol{\tau}, \boldsymbol{v}, q) \end{cases} \tag{13}$$

where $\mathcal{A}$ is the bilinear form defined on $V \times V \to \mathbb{R}$ as follows

$$\begin{aligned} \big\langle \mathcal{A}(\boldsymbol{\sigma}^k, \boldsymbol{u}^k, p^k)(\boldsymbol{\sigma}, \boldsymbol{u}, p), (\boldsymbol{\tau}, \boldsymbol{v}, q) \big\rangle &= \int_\Omega \big(\boldsymbol{\sigma} + p\mathbf{I} - 2\nu\mathbf{D}(\boldsymbol{u})\big) : \big(\boldsymbol{\tau} + q\mathbf{I} - 2\nu\mathbf{D}(\boldsymbol{v})\big)\, d\Omega \\ &+ \int_{\Gamma_N} \big(\boldsymbol{n}\cdot\boldsymbol{\sigma}\big)\cdot\big(\boldsymbol{n}\cdot\boldsymbol{\tau}\big)\, ds + \int_\Omega \big(\nabla\cdot\boldsymbol{u}\big)\big(\nabla\cdot\boldsymbol{v}\big)\, d\Omega \\ + \int_\Omega \big(\boldsymbol{u}\cdot\nabla\boldsymbol{u}^k + \boldsymbol{u}^k\cdot\nabla\boldsymbol{u} &+ \nabla\cdot\boldsymbol{\sigma}\big)\cdot\big(\boldsymbol{v}\cdot\nabla\boldsymbol{u}^k + \boldsymbol{u}^k\cdot\nabla\boldsymbol{v} + \nabla\cdot\boldsymbol{\tau}\big)\, d\Omega \end{aligned} \tag{14}$$

and the bilinear form $\mathcal{F}$ is defined on $V \to \mathbb{R}$ as follows:

$$\mathcal{F}(\boldsymbol{\sigma}^k, \boldsymbol{u}^k, p^k)(\boldsymbol{\tau}, \boldsymbol{v}, q) = \int_\Omega \left(\frac{\partial\mathcal{R}(\boldsymbol{\sigma}^k, \boldsymbol{u}^k, p^k)}{\partial x}(\boldsymbol{\tau}, \boldsymbol{v}, q)\right)\cdot\left(\mathcal{R}(\boldsymbol{\sigma}^k, \boldsymbol{u}^k, p^k)\right) d\Omega \tag{15}$$

2.5 Operator Form of the Problem

To analyze the properties of the least-squares problem, let us write the bilinear form (14) as in (10). Then, the S-V-P operator reads:

$$\begin{aligned} \mathcal{A}(\boldsymbol{\sigma}, \boldsymbol{u}, p) &= \left[\frac{\partial\mathcal{R}(\boldsymbol{\sigma}, \boldsymbol{u}, p)}{\partial x}\right]^* \left[\frac{\partial\mathcal{R}(\boldsymbol{\sigma}, \boldsymbol{u}, p)}{\partial x}\right] \\ &= \begin{pmatrix} \mathbf{I} - \nabla\nabla\cdot + \boldsymbol{n}_{\Gamma_N}\boldsymbol{n}_{\Gamma_N}\cdot & -2\nu\mathbf{D} - \nabla C(\boldsymbol{u}) & I \\ 2\nu\nabla\cdot + C^*(\boldsymbol{u})\nabla\cdot & -4\nu^2\nabla\cdot\mathbf{D} - \nabla\nabla\cdot + C^*(\boldsymbol{u})C(\boldsymbol{u}) & 2\nu\nabla\cdot \\ \mathbf{I} & -2\nu\mathbf{D} & I \end{pmatrix} \end{aligned} \tag{16}$$

Here, the nonlinear term $C(\boldsymbol{u})$ is defined as follows:

$$\langle C(\boldsymbol{u}), v\rangle = \int_\Omega \boldsymbol{v}\cdot\nabla\boldsymbol{u} + \boldsymbol{u}\cdot\nabla\boldsymbol{v}\, d\Omega \tag{17}$$

The resulting matrix, from equations (16), is symmetric and positive definite. So, after discretization, we are able to use the CG method to efficiently solve the system of equations. Our aim is to design an efficient solver which exploits the properties of the least-squares system with respect to both the CG and the multigrid methods. Therefore, we use CG as the main solver and accelerate it with the multigrid preconditioning.

2.6 Discrete Least-Squares Principle

Let the bounded domain $\Omega \subset \mathbb{R}^d$ be partitioned by a *grid* $\mathcal{T}_h$ consisting of elements $K \in \mathcal{T}_h$ which are assumed to be open quadrilaterals or hexahedrons such that $\Omega = \operatorname{int}\big(\bigcup_{K\in\mathcal{T}_h} \overline{K}\big)$. Furthermore, let $H^{1,h}(\Omega)$, $H^{s,h}(\Omega)$, and $H^{\mathrm{div},h}(\Omega)$ denote the spaces of elementwise H^1, H^s, and $H(\mathrm{div})$ functions with respect to $\mathcal{T}_h$ [2].

Now, we turn to the approximation of the problem (13) with the finite element method. So, we introduce the approximation spaces V^h such that

$$V^h \subset \mathbf{H}^{\mathrm{div},h}(\Omega) \cap \mathbf{H}^{s,h}(\Omega) \times \mathbf{H}^{1,h}_{g_D,D}(\Omega) \times L^2_0(\Omega) \tag{18}$$

and we consider the approximated problems

$$\begin{cases} Find\,(\boldsymbol{\sigma}_h, \boldsymbol{u}_h, p_h) \in V^h \quad s.t. \\ \langle \mathcal{A}^h(\boldsymbol{\sigma}, \boldsymbol{u}, p), (\boldsymbol{\tau}_h, \boldsymbol{v}_h, q_h)\rangle = \mathcal{F}^h(\boldsymbol{\tau}_h, \boldsymbol{v}_h, q_h) \end{cases} \tag{19}$$

where $\mathcal{A}^h$ is an approximate bilinear form of (14) defined on $V^h \times V^h \to \mathbb{R}$.

The least-squares formulation allows a free choice of FE spaces [4]. So, we are able to use different combinations of FE approximations, as for instance, discontinuous P_0^{dc}, P_1^{dc}, H^1-nonconforming $\tilde{Q}_1$ and $\tilde{Q}_2$, H^1-conforming Q_1 and Q_2, or from $H(\mathrm{div})$. Here we use different combinations of finite element spaces allowing better comparison with the standard mixed finite element for velocity and pressure. Therefore, we set $V^h \subset V$, and $\mathcal{A}^h = \mathcal{A}$.

2.7 MPCG Solver

The discrete linear system of equations resulting from the least-squares finite element method (16) has a symmetric and positive definite (SPD) coefficient matrix i.e.

$$\mathcal{A} = \begin{pmatrix} A_{\boldsymbol{\sigma}\boldsymbol{\sigma}} & A_{\boldsymbol{\sigma}\boldsymbol{u}} & A_{\boldsymbol{\sigma}p} \\ A_{\boldsymbol{\sigma}\boldsymbol{u}} & A_{\boldsymbol{u}\boldsymbol{u}} & A_{\boldsymbol{u}p} \\ A_{\boldsymbol{\sigma}p} & A_{\boldsymbol{u}p} & A_{pp} \end{pmatrix} \tag{20}$$

Therefore, it is appropriate to take full advantage of the symmetric positive definiteness by using solvers specially designed for such systems. In addition, the resulting system matrix is sparse due to the properties of the interpolation functions used in the finite element discretization. Our main focus is on the iterative solvers. We specifically employ the conjugate gradient method as a Krylov subspace solver suitable for the SPD systems. In addition, we use multigrid method as a highly efficient defect correction scheme for sparse linear systems arising in the discretization of (elliptic) partial differential equations [3].

3 Numerical Results and Discussions

We investigate the performance of the MPCG solver for the system (20) for a wide range of parameters, using the benchmarks quantities drag, lift, pressure drop, and the Global Mass Conservation (GMC) (see [3]). Moreover, we analyze the performance of the MPCG solver for the solution of the S-V-P. Figure 1 shows the computational mesh of the coarsest level.

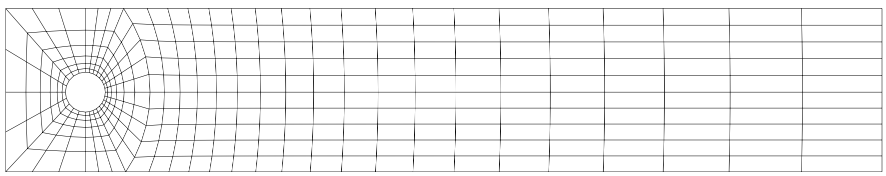

Fig. 1. Flow around cylinder: computational grid on level 1

Table 1. S-V-P Formulation: Benchmark quantities for flow around cylinder at $\mathsf{Re} = 20$.

	Level	d.o.f.	C_D	C_L	$\triangle p$	$GMC_{\vert x=2.2}$	NL/MG
$Q_1/Q_1/Q_1$	4	22,144	5.1716353	0.0210522	0.0103135	1.114501	7/19
	5	88,576	5.4440131	0.0142939	0.1117922	0.299773	7/17
	6	354,304	5.5415463	0.0117584	0.1152451	0.077866	7/17
$Q_2/Q_2/Q_2$	3	135,024	5.5588883	0.0101360	0.1165546	0.022791	6/12
	4	535,776	5.5769755	0.0105355	0.1173265	0.003022	6/12
	5	2,134,464	5.5792424	0.0106064	0.1174766	0.000556	6/12
$Q_2/Q_2/P_1^{\mathrm{dc}}$	3	129,128	5.5586141	0.0101405	0.1168068	0.0320698	6/13
	4	512,912	5.5769573	0.0105351	0.1173867	0.0039341	6/13
	5	2,044,448	5.5792414	0.1060618	0.1174911	0.0004692	6/13
ref.:		$C_D = 5.57953523384, C_L = 0.010618948146, \triangle p = 0.11752016697$					

We present the drag and the lift coefficients, the pressure drop across the cylinder, and the $GMC_{\vert x=2.2}$ values at the outflow ($x = 2.2$) at Reynolds number $\mathsf{Re} = 20$ for the S-V-P formulation in Table 1 which also shows the number of nonlinear iterations and the corresponding averaged linear solver (MPCG solver) iterations for different levels.

Using higher order finite elements, the method shows excellent convergence towards the reference solution. We observe a grid-independent convergence behavior.

4 Summary

We presented a numerical study regarding the accuracy and the efficiency of least-squares finite element formulation of the incompressible Navier-Stokes equations. The first-order system is introduced using the stress, velocity, and pressure, known as the S-V-P formulation. We investigated different finite element spaces of higher and low order. Using the Newton scheme, the linearization is performed on the continuous operators. Then, the least-squares minimization is applied. The resulting linear system is solved using an extended multigrid-preconditioned conjugate gradient solver. The flow accuracy and the mass conservation of the LSFEM formulations are investigated using the incompressible steady-state laminar ‘flow around cylinder’ problem’.

On the accuracy aspect, we have shown that highly accurate results can be obtained with higher order finite elements. More importantly, we have obtained more accurate results with the higher-order finite elements with less number of degrees of freedom as compared to the lower-order elements. This obviously amounts to less computational costs. On the efficiency aspect, we have shown that the MPCG solver performs efficiently for LSFEM formulation.

Having the basic S-V-P LSFEM solver, our main objective is the investigation of generalized Newtonian fluids with the nonlinearity due to the stress $\boldsymbol{\sigma} = 2\nu(\dot{\gamma})\mathbf{D}(\boldsymbol{u}) - p\mathbf{I}$, and multiphase flow problems with the jump in the stress and discontinuous pressure.

Acknowledgement

This work was supported by the Mercator Research Center Ruhr (MERCUR) grant Pr-2011-0017, the DFG and STW through the grants DFG/STW: TU 102/44-1, and the HEC-DAAD program.

References

1. J. J. Heys, T. A. Manteuffel, S. F. McCormick, and L. N. Olson, *Algebraic multigrid for higher-order finite elements*, J. Comput. Phys. **204**:2 (2005), 520–532.
2. M. Köster, A. Ouazzi, F. Schieweck, S. Turek, and P. Zajac, *New robust nonconforming finite elements of higher order*, Applied Numerical Mathematics (2012), 166–184.
3. M. Nickaeen, A. Ouazzi, and S. Turek, *Newton multigrid least-squares FEM for the V-V-P formulation of the Navier-Stokes equations*, J. Comput. Phys. **256** (2014), 416 – 427.
4. P. Bochev and M. Gunzburger, *Least-squares finite element methods*, Springer, 2009.